Electromagnetic Emission Post Spinning Black Hole Magnetized Neutron Star Mergers

Shu-Qing Zhong[1,2] , Zi-Gao Dai[1,2] , and Can-Min Deng[3,4,5]

[1] School of Astronomy and Space Science, Nanjing University, Nanjing 210093, People's Republic of China; dzg@nju.edu.cn
[2] Key laboratory of Modern Astronomy and Astrophysics (Nanjing University), Ministry of Education, Nanjing 210093, People's Republic of China
[3] Department of Astronomy, School of Physical Sciences, University of Science and Technology of China, Hefei, Anhui 230026, People's Republic of China
dengcm@ustc.edu.cn
[4] CAS Key Laboratory for Research in Galaxies and Cosmology, Department of Astronomy, University of Science and Technology of China, Hefei 230026, Anhui, People's Republic of China
[5] School of Astronomy and Space Science, University Of Science And Technology Of China, Hefei, Anhui 230026, People's Republic of China

Abstract

For a binary composed of a spinning black hole (BH; with mass $\gtrsim 7M_\odot$) and a strongly magnetized neutron star (NS; with surface magnetic field strength $B_{\rm S,NS} \gtrsim 10^{12}\,{\rm G}$ and mass $\sim 1.4\,M_\odot$), the NS as a whole will possibly eventually plunge into the BH. During the inspiral phase, the spinning BH could be charged to the Wald charge quantity $Q_{\rm W}$ until merger in an electro-vacuum approximation. During the merger, if the spinning charged BH creates its own magnetosphere due to an electric field strong enough for pair cascades to spark, the charged BH would transit from electro-vacuum to force-free cases and could discharge in a time $\gtrsim 1$ ms. As the force-free magnetosphere is full of a highly conducting plasma, the magnetic flux over the NS's caps would be retained outside the BH's event horizon under the frozen-in condition. Based on this scenario, we here investigate three possible energy-dissipation mechanisms that could produce electromagnetic (EM) counterparts in a time interval of the BH's discharge post a BH–NS merger-induced gravitational wave event: (1) magnetic reconnection at the BH's poles would occur, leading to a millisecond bright EM signal, (2) a magnetic shock in the zone of closed magnetic field lines due to the detachment and reconnection of the entire BH magnetic field would probably produce a bright radio emission, e.g., a fast radio burst, and (3) the Blandford–Znajek mechanism would extract the BH's rotational energy, giving rise to a millisecond-duration luminous high-energy burst. We also calculate the luminosities due to these mechanisms as a function of BH's spin for different values of $B_{\rm S,NS}$.

Key words: stars: black holes – gravitational waves – stars: neutron – radiation mechanisms: non-thermal

1. Introduction

Eleven gravitational wave (GW) events have been observed from 10 black hole–black hole (BH–BH) mergers and one neutron star–neutron star (NS–NS) merger in the observing runs 1 and 2 (O1 and O2) of the Advanced LIGO and Virgo detectors (The LIGO Scientific Collaboration et al. 2018), including GW150914 (Abbott et al. 2016). The first NS–NS merger, GW170817, jointly detected with GW and electromagnetic (EM) radiation, has been a watershed event (Abbott et al. 2017a, 2017b, 2017c), which was accompanied by a weak short gamma-ray burst (GRB) 170817A, an early multiwavelength kilonova AT2017gfo (Coulter et al. 2017; Villar et al. 2017), and a late broadband afterglow (Goldstein et al. 2017; Hallinan et al. 2017; Savchenko et al. 2017; Troja et al. 2017; von Kienlin et al. 2017; Lyman et al. 2018; Margutti et al. 2018; Piro et al. 2019). However, what has not yet been formally observed is a BH–NS merger, even though a candidate GW event S190426c in O3 running was presented (LIGO Scientific Collaboration & Virgo Collaboration 2019), in which no evidence for follow-up EM counterparts was uncovered recently (Hosseinzadeh et al. 2019).

During a BH–NS merger, theoretically, the NS would be effectively tidally disrupted if the tidal radius ($R_{\rm tidal}$) is larger than the innermost stable circular orbit (ISCO, $R_{\rm ISCO}$) of the BH, $R_{\rm tidal} > R_{\rm ISCO}$ (or the BH–NS mass ratio, $q \equiv M_{\rm BH}/M_{\rm NS} \lesssim 5$) (Shibata et al. 2009; Bartos et al. 2013). The disrupted materials would be left behind outside the final BH remnant but some of them would fall back, generating a short GRB (Paczynski 1991) and an afterglow (Sari et al. 1998), accompanied by a radioactively powered kilonova, just as in the case of an NS–NS merger

(Li & Paczyński 1998; Fernández & Metzger 2016; Metzger 2017). If the mass ratio $q \gtrsim 5$, however, it is generally thought that the NS would plunge into the BH as a whole, leaving behind neither any material outside the BH remnant nor any significant EM emission.

Nevertheless, several possible scenarios have been proposed to produce EM counterparts prior to plunging BH–NS mergers. First, a BH battery power due to a spinning BH–magnetized NS (or nonspinning BH–spinning magnetized NS) binary inspiral behaving analogously to a unipolar inductor can serve as an energy source to generate EM emission such as a fast radio burst (FRB) or a relativistic fireball as long as the NS is strongly magnetized (McWilliams & Levin 2011; D'Orazio & Levin 2013; Mingarelli et al. 2015; D'Orazio et al. 2016). Second, if at least one of the members in a BH–NS binary is charged, such a binary could make an FRB or a short GRB through electric dipole radiation and magnetic dipole radiation (Zhang 2016, 2019a; Deng et al. 2018). Third, if the BH is highly spinning and immersed in a strongly magnetic field of the NS, the BH could be charged through the Wald's mechanism (Wald 1974) as a BH pulsar (Levin et al. 2018), and could create EM counterparts such as short X/γ-ray signals due to magnetic reconnection in addition to electric dipole radiation and magnetic dipole radiation (Dai 2019), as in the cases of binary BH mergers (Fraschetti 2018) and binary NS mergers (Wang et al. 2018).

Moreover, it has been argued that EM counterparts could be produced after a plunging BH–NS merger. If the binary includes a nonspinning BH and a spinning magnetized NS, a "blitzar" FRB would occur via a magnetic shock because of the "no-hair"

theorem (Falcke & Rezzolla 2014; Mingarelli et al. 2015). On the other hand, for a spinning BH–magnetized NS binary, the "no-hair" theorem could not be applicable formally and the magnetic flux at the plunging NS polar caps would be retained in the highly conducting plasma outside the BH's event horizon during the resistive timescale of the magnetosphere (Lyutikov & McKinney 2011), so that a type of afterglow post BH–NS merger would be powered via the Blandford–Znajek (BZ) mechanism (Blandford & Znajek 1977; D'Orazio et al. 2016).

During the inspiral of a spinning massive BH–magnetized NS binary, the BH could be charged because it is immersed in the magnetosphere of the NS, so that this system would become a spinning charged BH–magnetized NS binary. Its premerger energy-dissipation mechanisms such as magnetic reconnection, electric dipole radiation, and magnetic dipole radiation could give rise to EM emission (Dai 2019). In this Letter, we investigate postmerger possible mechanisms to generate EM counterparts that are suitable for a spinning massive BH–magnetized NS binary in which the BH is charged via the Wald process, based on the previously studied scenarios in some binary systems, e.g., a spinning charged BH–magnetized NS binary premerger, a nonspinning BH–spinning magnetized NS binary postmerger, and a spinning BH–magnetized NS binary postmerger. Ultimately, we find that three possible mechanisms such as magnetic reconnection, magnetic shock, and BZ mechanism are interesting. This paper is organized as follows. In Section 2 we briefly illustrate the schematic picture of these three mechanisms. In Section 3, we calculate the emission luminosities due to the mechanisms. Finally, we present a discussion and summary in Section 4.

2. Processes Post a Magnetized NS Plunging into a Spinning BH

For convenience of numerical calculations, we show the quantities in cgs units. We use a subscript "NS" to indicate the quantities of an NS (those without subscript "NS" are the BH's). For a spinning BH–magnetized NS binary in an electro-vacuum approximation, as shown in Levin et al. (2018), the BH could not only be charged stably but also maintain the Wald's charge quantity $Q = Q_W$ until the NS plunges into the BH, even though EM emission during the charging process and continual flux of charges within the BH–NS system occurs. During this plunging period, as the separation between BH and NS reaches the NS's radius ($r \rightarrow R_{NS}$), Wald's maximal charge quantity of the BH is

$$Q_{W,max} \simeq \frac{2G}{c^3} J \times B_{S,NS} = \frac{2G^2}{c^4} a M^2 B_{S,NS}$$

$$= 4.4 \times 10^{24} a \left(\frac{M}{10 M_\odot} \right)^2 \frac{B_{S,NS}}{10^{12} G} \text{ e.s.u.,} \quad (1)$$

where J, $a = Jc/GM^2$, M, and $B_{S,NS}$ are the BH's angular momentum, dimensionless spin parameter, mass, and the NS's surface magnetic dipole field strength, respectively. The Wald charge would give rise to a magnetic dipole field of the BH whose strength at any radius r is (Levin et al. 2018; Dai 2019)

$$B_W = \frac{J Q_{W,max}}{Mcr^3} = \frac{2G^3}{c^6} a^2 M^3 B_{S,NS} r^{-3}$$

$$= 6.5 \times 10^{12} a^2 \left(\frac{M}{10 M_\odot} \right)^3 \left(\frac{B_{S,NS}}{10^{12} \text{ G}} \right) \left(\frac{r}{10^6 \text{ cm}} \right)^{-3} \text{ G.} \quad (2)$$

During the merger, if the spinning charged BH creates its own magnetosphere due to an electric field strong enough for pair cascades to spark, the charge BH would transit from electro-vacuum to force-free cases. This does not mean that the BH would completely discharge immediately. As shown in Pan & Yang (2019), the duration of BH discharge may be larger than the light-crossing time ~1 ms. However, if the resistive time of a force-free magnetosphere is considered (Lyutikov & McKinney 2011), the duration of BH discharge could be longer. This duration is comparable to the duration of the mechanisms that we discuss below. So these mechanisms would occur even if the BH discharge takes place in the postmerger force-free case.

In the scenario discussed above, on one hand, no matter whether the BH spin aligns or anti-aligns with the NS magnetic axis before the NS is swallowed, the BH's magnetic dipole field created from the spinning electric charge inside the BH event horizon is always anti-parallel to that of the NS (Dai 2019), so a magnetic reconnection event could occur in an interacting field zone close to the BH equatorial plane initially (Dai 2019), as in the case of a binary NS premerger (Wang et al. 2018). During the NS plunging into the BH, the NS's closed magnetic field lines would be swallowed together with the NS, while the open field lines which originally connect the NS's polar surface to infinity also connect the BH's event horizon to infinity because of the frozen-in condition of a highly conducting plasma, which is akin to the cases in a rotating NS collapsing to a slowly balding BH (Lyutikov & McKinney 2011) or in a strongly magnetized NS-Kerr BH binary postmerger (D'Orazio et al. 2016). Therefore, the magnetic reconnection zone close to the BH's equatorial plane premerger in Dai (2019) would be transferred to the BH polar regions postmerger, in which regions the open field lines of the BH would reconnect with those of the NS.

On the other hand, the BH discharge process, just like the magnetosphere collapse due to the magnetosphere instability proposed in Liu et al. (2016), would in principle result in an entire magnetic field detachment and reconnection, which generates a strong magnetic shock at the speed of light to sweep up the magnetosphere plasma, similar to the mechanism for a supramassive the NS collapsing to a BH,[6] proposed by Falcke & Rezzolla (2014). In addition, the third mechanism— BZ mechanism may occur to extract the BH's rotational energy, as in the case of a strongly magnetized NS-Kerr BH binary postmerger (D'Orazio et al. 2016). The schematic picture for these processes is shown in Figure 1.

3. Mechanisms of EM Emission Postmerger

3.1. Magnetic Reconnection

The magnetic reconnection would be transferred from the region close to the BH's equatorial plane premerger to the polar regions postmerger. The energy of each pole at radius $r - r + dr$

$$dE_{REC}(r) = \frac{B_W^2}{8\pi} dV_p(r), \quad (3)$$

can be dissipated, where $dV_p(r)$ is the volume in an interval of r to $r+dr$. Based on Equations (1) and (2), the magnetic field at

---

[6] A strong magnetic shock wave is seen in 3D resistive MHD simulations on the collapse of nonrotating NSs (Dionysopoulou et al. 2013).
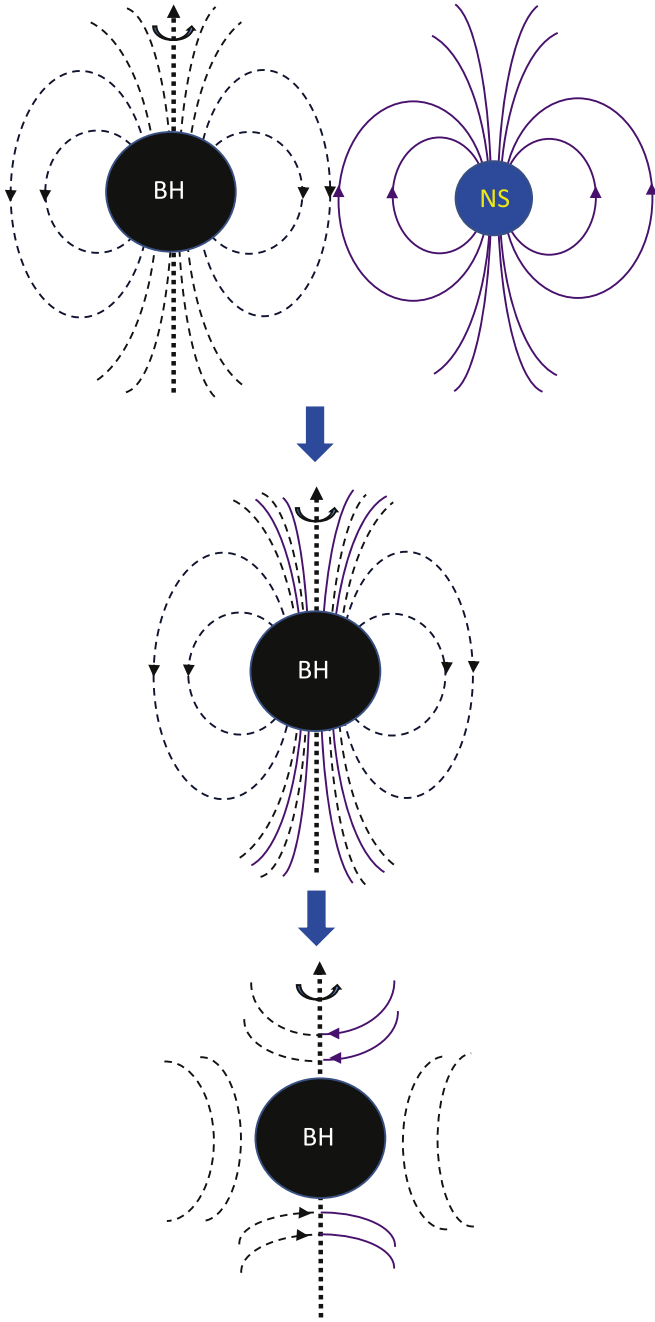
Figure 1. Schematic picture of a plunging spinning BH–magnetized NS binary premerger and postmerger (for convenience, we just show some of the magnetic field lines of the NS in the top panel. In reality, the farthest closed magnetic field lines of the NS should already thread the BH since the BH immersed in the NS's magnetosphere could be charged). Prior to the merger, the spinning BH would not only be charged stably up to the Wald charge Q_W but also maintain it up to its maximum quantity in an electro-vacuum approximation. During the merger, if the spinning charged BH creates its own magnetosphere due to an electric field strong enough for pair cascades to spark, the charge BH would transit from electro-vacuum to force-free cases. Furthermore, during the NS plunging into the BH, the NS's closed magnetic field lines would be swallowed together with the NS, while the open field lines which originally connect the NS's polar surface to infinity also connect the BH's event horizon to infinity because of the frozen-in condition of a highly conducting plasma. In this scenario, on one hand, the open magnetic field lines of the BH at polar regions would reconnect with those of the NS because the BH magnetic dipole field lines are always anti-parallel to those of the NS. On the other hand, the BH's discharge might create a magnetic shock due to the detachment and reconnection of the entire magnetic field of the BH, leading to the magnetosphere plasma dissipation. In addition, the third process—BZ mechanism may occur to extract the BH's rotational energy.

the BH's horizon radius (Misner et al. 1973)

$$R_H = \frac{GM}{c^2} + \sqrt{\frac{G^2M^2}{c^4} - \frac{G^2M^2}{c^4}a^2 - \frac{GQ_{W,max}^2}{c^4}}$$

$$\approx \frac{GM}{c^2} + \sqrt{\frac{G^2M^2}{c^4} - \frac{G^2M^2}{c^4}a^2}, \qquad (4)$$

can reach 10^{11} G for the BH mass $\sim 10 M_\odot$, the NS's surface magnetic field strength $\sim 10^{12}$ G, and the spin parameter $a \sim 0.6$. Hence, for a relatively low BH spin $a < 0.6$, the strength of BH's horizon magnetic field is much smaller than the surface magnetic field of the NS. In this case, the BH's open magnetic field lines can only reconnect a small part of the open magnetic field lines of the NS. We next calculate the volume $dV_p(r)$ with an analogy to that of a pulsar

$$dV_p(r) = A(r)dr, \qquad (5)$$

where $A(r) = \pi r^2 \sin^2\theta \sim \pi r^2 R_H/R_{LC}$, and R_{LC} is the light cylinder radius of the BH. Here any dipole magnetic field line satisfies $r' = r'_{max}\sin^2\theta$, where $r' \sim R_H$ and $r'_{max} \sim R_{LC}$ are adopted (Piro & Ott 2011; Wang et al. 2018).

The light cylinder radius can be written as

$$R_{LC} = c/\Omega, \qquad (6)$$

where the angular velocity is approximated as that close to the event horizon (see Equation (5) of Liu et al. 2016)

$$\Omega = \frac{GMa}{c[R_H^2 + (GMa/c^2)^2]}. \qquad (7)$$

From Equations (1)–(3), (5), and (6), one can obtain the total magnetic reconnection energy for each polar region

$$E_{REC} = \int_{R_H}^{R_{LC}} \frac{B_W^2}{8\pi}\frac{R_H}{R_{LC}}\pi r^2 dr \approx \frac{G^6 a^4 M^6 B_{S,NS}^2}{6c^{12}}\frac{1}{R_H^2 R_{LC}}, \qquad (8)$$

which can be as a function of the spin parameter a for different NS's surface magnetic fields $B_{S,NS} = 10^{12}$, 10^{14}, and 10^{16} G, and BH mass $M = 10 M_\odot$, displaying in panel (a) of Figure 2. The magnetic reconnection energy rises with increasing the NS's surface magnetic field and the BH spin.

If the magnetic reconnection dissipation timescale is assumed to be the Alfvén propagation timescale t_A, this timescale can be expressed as the ratio of the light cylinder of the BH (R_{LC}) to the Alfvén speed (v_A)

$$t_A = \frac{R_{LC}}{v_A}, \qquad (9)$$

where v_A can be generally expressed by (see Equation (2.11a) in Punsly 1998)

$$v_A = \frac{U_A}{\gamma_A} = \frac{B_W}{\gamma_A\sqrt{4\pi n_e \mu}}c, \qquad (10)$$

where n_e is the particle number density in the BH's magnetosphere, U_A is the pure Alfvén speed and $\gamma_A = \frac{1}{\sqrt{1 - v_A^2/c^2}}$, and
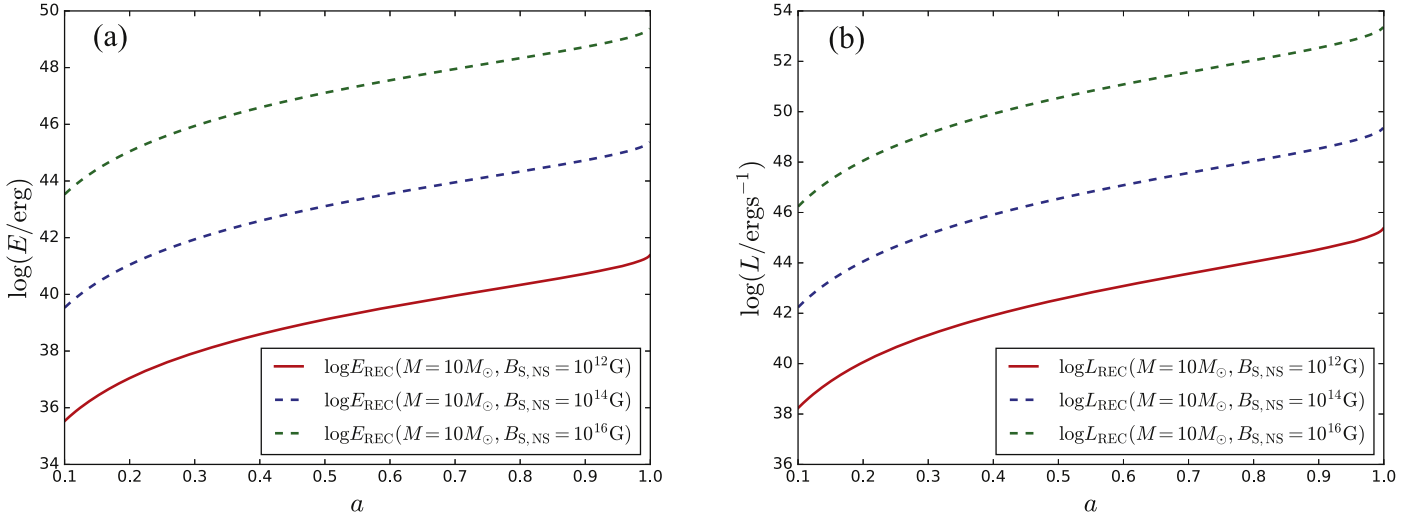
Figure 2. Panels (a) and (b): the magnetic reconnection energy E_{REC} at each BH's pole and the corresponding luminosity L_{REC} as a function of BH dimensionless spin parameter a for different $B_{S,NS}$.

$\mu \sim 10^{-6}$ is the plasma specific enthalpy in units of the electron's rest mass energy.[7] The particle number density n_e in the KNBH's magnetosphere is unlikely to be calculated accurately due to complexity of the magnetosphere, even though a KNBH's magnetosphere model with a magnetically dominated plasma has been explored in Punsly (1998). In his model, the particle number density is nonlinear and uncertain no matter the MHD wind zone and the zone of closed magnetic field lines of the magnetosphere, even though it has been simplified under several assumptions. This may be why Liu et al. (2016) did not adopt this magnetosphere model to calculate the particle number density for a KNBH. Instead, Liu et al. (2016) took n_e to be a factor k times the Goldreich–Julian density (Goldreich & Julian 1969; as done in Falcke & Rezzolla 2014)

$$n_e = k \frac{B_W \Omega}{2\pi c e}, \tag{11}$$

where k is uncertain but it is assumed to be typically of order unity here, $k \sim O(1)$. In the following, we always take $k = 1$. This assumption seems to be reasonable based on the model of Punsly (1998), in which the particle number density has a basically similar but more complicated form associated with the magnetic field strength and angular velocity of the BH no matter the MHD wind zone or the zone of closed magnetic field lines of magnetosphere (see Equations (4.12a) and (A.12) in Punsly 1998). From Equations (10) and (11), the Alfvén speed can be also written as $v_A = \frac{B_W^{1/2}\Omega^{-1/2}c}{\gamma_A \sqrt{2k\mu/ce}}$, which implies that the Alfvén speed close to R_{LC} is smaller than that close to the BH horizon. Thus, we use the Alfvén speed close to R_{LC} to

represent the Alfvén speed of the magnetosphere. Hence, if $B_{S,NS} = 10^{12}$ G, $M = 10M_\odot$, and $a \sim 0.1-1.0$, then we obtain $B_W \gtrsim 10^5$ G for the whole magnetosphere ranging from R_H to R_{LC} and v_A basically equals the speed of light c. Moreover, the stronger NS's magnetic field corresponds to the higher Alfvén speed, as seen from the expression of v_A depending on B_W and Equation (2). Using $a = 0.1-1.0$ and $M = 10M_\odot$, we further get the BH magnetosphere size $R_{LC} \sim 3 \times 10^6-6 \times 10^7$ cm by combining Equations (6) and (7), so the Alfvén propagation timescale $t_A \sim 0.1 - 2$ ms. Moreover, in terms of Equations (1), (2), (6),(7), (8), (9), and (10), the total magnetic energy in each polar region of BH would be dissipated as a luminosity $L_{REC} = E_{REC}/t_A$, illustrated in panel (b) of Figure 2. The luminosity increases with increasing the BH spin and NS's surface magnetic field strength. Furthermore, it is comparable to the luminosity in a magnetic reconnection event close to the equatorial plane from the magnetospheres' contact of two NSs with a surface magnetic field 10^{12} G premerger (in case 1 in Figure 2 of Wang et al. 2018), only if the BH spin $a \gtrsim 0.6$.

3.2. Magnetic Shock

After the NS is swallowed, the spinning charged BH would discharge in a force-free approximation in an time interval $\gtrsim 1$ ms and then the entire BH magnetic field should detach and reconnect outside the horizon. This could generate a strong magnetic shock wave sweeping up the magnetosphere plasma at the speed of light. If the magnetic shock wave energy mainly arises from the magnetic energy in the zone of closed magnetic field lines, the total magnetic energy can be estimated by

$$E_{MS} = \int_{R_H}^{R_{LC}} \frac{B_W^2}{8\pi} 4\pi r^2 dr - 2E_{REC}$$
$$\approx \frac{G^6 a^4 M^6 B_{S,NS}^2}{3c^{12}} \left(\frac{2}{R_H^3} - \frac{1}{R_H^2 R_{LC}} \right), \tag{12}$$

which rises with increasing the NS's surface magnetic field and the BH's spin, shown in panel (a) of Figure 3.

---

[7] The quantity μ is calculated based on the assumption that the plasma is cold. μ is composed of the energy density ρ and the pressure P, where ρ consists of the corresponding energy of the rest mass ($m_e c^2$) and the internal energy I per particle. The internal energy per particle (I) is basically the random kinetic energy for an ordered EM field as was done here. The field-aligned acceleration produces an ordered field-aligned motion and does not produce a random kinetic energy so that it does not affect the internal energy per particle. The collision rate affects P and I, in a relatively low density approximation that both P and I are small compared to $m_e c^2$ (see Equation (2.13) in Punsly 2001).

Falcke & Rezzolla (2014) suggested that curvature radiation of the shock-accelerated electrons is possibly involved in the entire emission since processes like synchrotron radiation or self-absorption are not applicable because the gyro radius of the electrons are so small that the electrons will move essentially along the magnetic field lines. Accordingly, we consider curvature radiation in our scenario.

For the electron acceleration in the BH's magnetosphere postmerger, there are some approaches such as BH's electric field, compared to the voltage drop accelerating electrons across magnetic field lines connecting the NS to the BH premerger in McWilliams & Levin (2011) and D'Orazio et al. (2016). The curvature radiation power for an electron with Lorentz factor γ is

$$P_e = 2\gamma^4 e^2 c / 3 R_{\rm LC}^2, \qquad (13)$$

its corresponding characteristic frequency

$$\nu_c = \frac{3}{4\pi} \frac{c\gamma^3}{R_{\rm LC}} \approx 7\gamma^3 \left(\frac{R_{\rm LC}}{10^6 \, {\rm cm}}\right)^{-1} {\rm kHz}. \qquad (14)$$

Due to the aforementioned BH magnetosphere size $R_{\rm LC} \sim 3 \times 10^6$–$6 \times 10^7$ cm, the duration of the shock wave sweeping up the magnetosphere would be $\sim$0.1–2 ms, which coincides with the typical duration of an FRB. Additionally, for a relativistic electron accelerated to a Lorentz factor $\gamma \sim 100$, the characteristic curvature radiation frequency is $\nu_c \sim$ GHz, falling into the FRB's frequency range. Based on Equation (11), the average electron number density can be approximated by $\bar{n}_e \approx \frac{\int_{R_{\rm H}}^{R_{\rm LC}} 4\pi n_e r^2 dr}{V_{\rm LC}}$, where $V_{\rm LC} = \frac{4}{3}\pi(R_{\rm LC}^3 - R_{\rm H}^3) \approx \frac{4}{3}\pi R_{\rm LC}^3$ is the volume of the whole BH magnetosphere. As long as the NS's surface magnetic field $B_{\rm S,NS} < 10^{14}$ G, the curvature radiation frequency of an electron with $\gamma \sim 100$ would be well above the surrounding plasma frequency $\nu_p = \gamma^{-3/2}(4\pi \bar{n}_e e^2/m_e)^{1/2}$, as shown in panel (b) of Figure 3.

According to the analysis of Falcke & Rezzolla (2014), the characteristic length of curvature radiation is a few 10^7 cm, comparable with the size of the shock wave—the magnetosphere size if the Lorentz factor of charges $\gamma \sim 1$. Under this condition, the entire emission would be coherent. However, for electrons with higher Lorentz factors (e.g., $\gamma \sim 100$), their coherence length would become much smaller than the magnetosphere size, so the coherently emitting region should become slices and the slice number is estimated by $N_{\rm slice} \simeq V R_{\rm LC}^{-2}(c/\nu_c)^{-1} = \gamma^3$. Thus the total emitted power becomes $P_{\rm tot} = \eta_e N_{\rm slice}^{-1} N_e^2 P_e = \eta_e N_{\rm slice}^{-1}(\bar{n}_e V)^2 P_e$ (where η_e accounts for a fraction of electrons that are accelerated to Lorentz factor γ). Therefore, the luminosity by coherent curvature radiation of electrons within the zone of closed magnetic field lines can be calculated by

$$L_{\rm CCR} = \eta_e [\bar{n}_e (V_{\rm LC} - 2V_p)]^2 P_e \gamma^{-3}, \qquad (15)$$

where $V_{\rm LC} - 2V_p$ is the volume of the zone of closed magnetic field lines and $V_p = \int_{R_{\rm H}}^{R_{\rm LC}} A(r) dr \approx \frac{\pi R_{\rm H}}{R_{\rm LC}}(R_{\rm LC}^3 - R_{\rm H}^3) \approx \pi R_{\rm H} R_{\rm LC}^2$. From Equations (1), (2), (6), (7), (13), (11), and (15), the luminosity can be estimated as a function of BH spin a for different NS's surface magnetic field strengths, plotted in panel (c) of Figure 3 (with $M = 10 M_\odot$, $\gamma = 100$, and $\eta_e = 0.05$). As we can see, the luminosity rapidly rises with increasing the NS's surface magnetic field and the BH spin. Moreover, it needs a low

spin regime to make the luminosity fall into the characteristic FRB luminosity 10^{42}–10^{44} erg s^{-1} (Zhang 2019a) if a high surface magnetic field of the NS is assumed.

This luminosity corresponds to the energy which is written by

$$E_{\rm CCR} \approx \frac{L_{\rm CCR} R_{\rm LC}}{c}, \qquad (16)$$

which also increases with increasing NS surface magnetic field and BH spin, illustrated in panel (d) of Figure 3. In comparison to the result in panel (a) of Figure 3, the energy dissipated via coherent curvature radiation of electrons is a significant fraction of the total magnetic energy in the zone of closed magnetic field lines.

If electrons are accelerated to a very large Lorentz factor, e.g., $\gamma \sim 10^7$ as argued in D'Orazio et al. (2016), their corresponding characteristic curvature radiation frequency would fall into GeV gamma-rays based on Equation (14). In this case, the curvature radiation is impossibly coherent, so the total power can be estimated by

$$L_\gamma = \eta_e \bar{n}_e (V_{\rm LC} - 2V_p) P_e. \qquad (17)$$

Adopting $\gamma = 10^7$ and $\eta_e = 1$, the luminosity as a function of BH spin for different NS surface magnetic fields is found in panel (e) of Figure 3. As we can see, this luminosity is very small compared to the luminosity of coherent curvature radiation for electrons with Lorentz factor $\sim$100, for the same fiducial parameter values. Moreover, it is noted that just a small fraction of ($\eta_e = 0.05$) electrons with $\gamma = 100$ has been assumed to account for a bright radio emission and that almost all ($\eta_e = 1$) electrons with $\gamma = 10^7$ only account for a faint high-energy transient. Accordingly, the magnetic shock sweeping up the magnetosphere plasma is more likely to generate a bright millisecond radio emission, e.g., an FRB, if the BH spin and the NS's surface magnetic field lie in appropriate regimes, rather than a high-energy (e.g., γ-ray) transient. Therefore, this mechanism associated with a plunging BH–NS merger event might be responsible for a fraction of nonrepeating FRBs.

3.3. BZ Mechanism

During the period of magnetic reconnection at BH's poles and BH discharge resulting in a magnetic shock, the BZ mechanism might operate to extract the BH's rotational energy since the charged BH has created its own vicinal magnetosphere pervaded with charged particles postmerger. According to D'Orazio et al. (2016), the BZ mechanism luminosity can be estimated by

$$L_{\rm BZ} \sim \frac{\phi^2}{4\pi c}\left(\frac{ac}{R_{\rm H}}\right)^2, \qquad (18)$$

where ϕ is the remaining open magnetic flux of the NS after the open magnetic field lines of the NS reconnect with those of the BH, which can be approximated by

$$\phi \sim 2\pi (B_{\rm NS} - B_{\rm H}) R_{\rm NS}^2 \sin^{-1}\left(\frac{R_{\rm NS}\Omega_{\rm orb}}{c}\right), \qquad (19)$$

where $B_{\rm H} = \frac{2G^3}{c^6} a^2 M^3 B_{\rm S,NS} R_{\rm H}^{-3}$ is the magnetic field strength at the BH's horizon from Equation (2) and $\Omega_{\rm orb}$ is the orbital
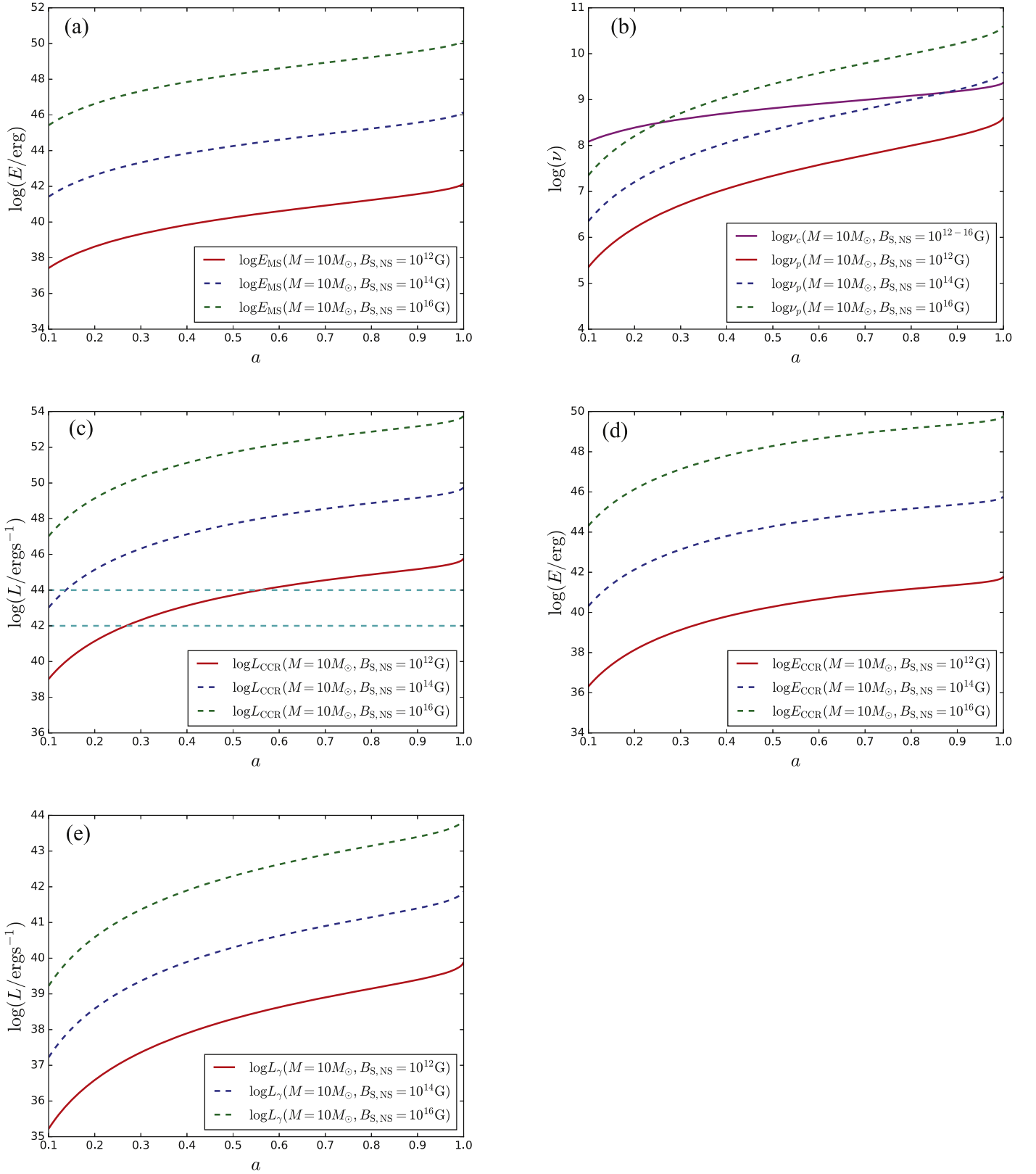
Figure 3. Panel (a): the total magnetic energy in the zone of closed magnetic field lines varies with the BH spin parameter for different $B_{S,NS}$. Panel (b): comparison between the characteristic curvature radiation frequency ν_c for a relativistic charge with $\gamma \sim 100$ and the plasma frequency ν_p for different $B_{S,NS}$. Panels (c) and (d): the total coherent curvature radiation luminosity and energy for electrons with $\gamma \sim 100$ resulted from the magnetic shock as a function of BH spin parameter for different $B_{S,NS}$. The cyan lines in panel (c) represent the range of a typical FRB luminosity. Panel (e): the total curvature radiation luminosity if electrons have $\gamma \sim 10^7$.
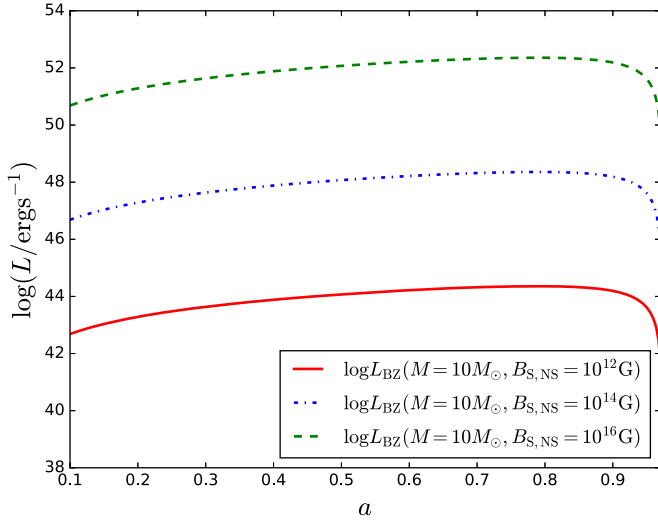
Figure 4. BZ luminosity as a function of BH dimensionless spin parameter for different $B_{S,NS}$.

angular velocity near the merger time (D'Orazio et al. 2016). Combining Equations (4), (18), and (19), we obtain the BZ luminosity as a function of BH spin a for the NS's surface magnetic fields $B_{S,NS} = 10^{12}$, 10^{14}, and 10^{16} G, with BH mass $M = 10 M_{\odot}$, NS radius $R_{NS} = 10^6$ cm, and $\frac{2\pi}{\Omega_{orb}} = 1$ ms, as shown in Figure 4. This figure shows that the BZ luminosity is comparable to that of Figure 6 in D'Orazio et al. (2016). However, there are some differences. For example, the luminosity is not sensitive to the BH spin because the magnetic field at the BH's horizon resulting from the Wald charge is very small compared to the corresponding NS's surface magnetic field until $a \sim 0.7$. Only when the spin is extremely high, $a > 0.9$, is the magnetic field strength at the BH's horizon comparable to the NS's surface magnetic field strength, so most of the open magnetic field lines of the NS can be reconnected by those of the BH, leading to the BZ luminosity that decays as the BH spin increases. This highly bright BZ luminosity could create a relativistic Poynting-flux-dominated jet along the rotational axis, which has a duration similar to the timescale of magnetic reconnection and BH discharge (i.e., ~1 ms). This jet would produce a high-energy (e.g., X-ray/γ-ray) transient due to internal magnetic dissipation in the optically thin region far away from the central engine (Lyutikov & Blandford 2003; Zhang & Yan 2011; Beniamini & Giannios 2017; Xiao & Dai 2017, 2019; Xiao et al. 2018).

4. Discussion and Summary

In a spinning massive BH–magnetized NS merger, the spinning BH could be charged to the maximal Wald charge quantity premerger in an electro-vacuum approximation. During the NS plunging into the BH, if the spinning charged BH could transit from electro-vacuum to force-free cases and discharge rapidly. During the BH's discharge, the magnetic reconnection, magnetic shock, and BZ process would probably occur, so that they might generate a millisecond luminous EM signal, a millisecond radio bight emission like an FRB, or a millisecond high-energy (X-ray/γ-ray) transient. Although the

three processes have distinct energy sources, it is unclear whether they would occur simultaneously. In addition, we see that if the BH has an extremely high spin $a > 0.9$, the BZ luminosity decreases with a. These mechanisms of generating postmerger EM emission should be also applicable to the merger of a spinning BH–charged BH binary, in which the spinning BH immersed in the magnetic field of the charged BH could be also charged via the Wald charging scenario at the final inspiral stage premerger.

In principle, there could be a time delay between the premerger emission and the postmerger emission, at least the sum of the time from the BH's ISCO to the BH–NS merger and the light-crossing time of the BH theoretically, e.g., $\gtrsim 0.5$ ms for BH mass $M = 10 M_{\odot}$ (Mingarelli et al. 2015). Thus, to resolve the postmerger FRBs, it requires at least the 0.5 ms resolution of a telescope. Fortunately, it is easy to identify an FRB that possibly resulted from a premerger inspiral or a postmerger process if the FRB arrives at an observer later than the GW emission during the merger. On the other hand, it is impossible to distinguish a postmerger high-energy transient from a premerger emission suggested by Dai (2019) observationally, if the delay between a premerger emission and a postmerger emission is as short as $\lesssim 1$ ms, compared with a possible long time delay between GW-GRB association (the time of launching a relativistic jet + the time for the jet to break out + the time for the jet to reach a GRB emission site) (Zhang 2019b), e.g., the premerger magnetic dipole radiation process in Zhang (2016) can also explain the 0.4 s time delay for the candidate GW150914/GW150914-GBM association (Connaughton et al. 2016, 2018; Greiner et al. 2016). However, it can be seen that two postmerger mechanisms, i.e., magnetic reconnection and magnetic shock discussed in this paper are nearly independent of the NS properties such as the mass and radius, except for its surface magnetic dipole field, which is different from the premerger mechanisms shown in Dai (2019).

If FRBs produced from the magnetic shock are not beamed and the plunging BH–NS merger rate density upper bound $\mathfrak{R}_{BH-NS} \lesssim 610 \, Gpc^{-3} yr^{-1}$ (The LIGO Scientific Collaboration et al. 2018), then the GW-FRB association rate density from plunging BH–NS mergers may be $\mathfrak{R}_{GW-FRB} \lesssim 610 \, Gpc^{-3} yr^{-1}$.

Finally, a different mechanism to produce EM emission during BH's discharge post a spinning massive BH–magnetized NS merger was investigated by Pan & Yang (2019), in which the electric energy could be released as high-energy gamma-rays through a cascade process in analogy to the mechanism of generating γ-ray emission in a radio pulsar (see Figure 2.2 in Beskin et al. 2004), for which primary electrons and positrons are accelerated in the BH electric field and then interact with surrounding soft photons created from cyclotron radiation by nonrelativistic electrons with the Goldreich–Julian density (Goldreich & Julian 1969) via inverse Compton scattering, and then resultant hard photons colliding with soft photons (or $\gamma + E/B \rightarrow e^+ + e^-$) will produce more and more energetic electrons and positrons as well as high-energy photons that would escape out of the magnetosphere.

ORCID iDs

Shu-Qing Zhong ⓘ https://orcid.org/0000-0002-1766-6947
Zi-Gao Dai ⓘ https://orcid.org/0000-0002-7835-8585

References

Abbott, B. P., Abbott, R., Abbott, T. D., et al. 2016, PhRvL, 116, 61102
Abbott, B. P., Abbott, R., Abbott, T. D., et al. 2017a, PhRvL, 119, 161101
Abbott, B. P., Abbott, R., Abbott, T. D., et al. 2017b, ApJL, 848, L13
Abbott, B. P., Abbott, R., Abbott, T. D., et al. 2017c, ApJL, 848, L12
Bartos, I., Brady, P., & Márka, S. 2013, CQGra, 30, 123001
Beniamini, P., & Giannios, D. 2017, MNRAS, 468, 3202
Beskin, V., Henri, G., Menard, F., et al. 2004, Accretion Discs, Jets and High
    Energy Phenomena in Astrophysics (New York: Oxford Univ. Press)
Blandford, R. D., & Znajek, R. L. 1977, MNRAS, 179, 433
Connaughton, V., Burns, E., Goldstein, A., et al. 2016, ApJL, 826, L6
Connaughton, V., Burns, E., Goldstein, A., et al. 2018, ApJL, 853, L9
Coulter, D. A., Foley, R. J., Kilpatrick, C. D., et al. 2017, Sci, 358, 1556
Dai, Z. G. 2019, ApJL, 873, L13
Deng, C.-M., Cai, Y., Wu, X.-F., et al. 2018, PhRvD, 98, 123016
Dionysopoulou, K., Alic, D., Palenzuela, C., et al. 2013, PhRvD, 88, 044020
D'Orazio, D. J., & Levin, J. 2013, PhRvD, 88, 64059
D'Orazio, D. J., Levin, J., Murray, N. W., et al. 2016, PhRvD, 94, 23001
Falcke, H., & Rezzolla, L. 2014, A&A, 562, A137
Fernández, R., & Metzger, B. D. 2016, ARNPS, 66, 23
Fraschetti, F. 2018, JCAP, 2018, 054
Goldreich, P., & Julian, W. H. 1969, ApJ, 157, 869
Goldstein, A., Veres, P., Burns, E., et al. 2017, ApJL, 848, L14
Greiner, J., Burgess, J. M., Savchenko, V., et al. 2016, ApJL, 827, L38
Hallinan, G., Corsi, A., Mooley, K. P., et al. 2017, Sci, 358, 1579
Hosseinzadeh, G., Cowperthwaite, P. S., Gomez, S., et al. 2019, ApJL,
    880, L4
Levin, J., D'Orazio, D. J., & Garcia-Saenz, S. 2018, PhRvD, 98, 123002

Li, L.-X., & Paczyński, B. 1998, ApJL, 507, L59
LIGO Scientific CollaborationVirgo Collaboration 2019, GCN, 24237, 1
Liu, T., Romero, G. E., Liu, M.-L., et al. 2016, ApJ, 826, 82
Lyman, J. D., Lamb, G. P., Levan, A. J., et al. 2018, NatAs, 2, 751
Lyutikov, M., & Blandford, R. 2003, arXiv:astro-ph/0312347
Lyutikov, M., & McKinney, J. C. 2011, PhRvD, 84, 84019
Margutti, R., Alexander, K. D., Xie, X., et al. 2018, ApJL, 856, L18
McWilliams, S. T., & Levin, J. 2011, ApJ, 742, 90
Metzger, B. D. 2017, LRR, 20, 3
Mingarelli, C. M. F., Levin, J., & Lazio, T. J. W. 2015, ApJL, 814, L20
Misner, C. W., Thorne, K. S., & Wheeler, J. A. 1973, Gravitation (San
    Francisco: W.H. Freeman and Co.)
Paczynski, B. 1991, AcA, 41, 257
Pan, Z., & Yang, H. 2019, PhRvD, 100, 043025
Piro, A. L., & Ott, C. D. 2011, ApJ, 736, 108
Piro, L., Troja, E., Zhang, B., et al. 2019, MNRAS, 483, 1912
Punsly, B. 1998, ApJ, 498, 640
Punsly, B. 2001, Black Hole Gravitohydromagnetics (New York: Springer), 37
Sari, R., Piran, T., & Narayan, R. 1998, ApJL, 497, L17
Savchenko, V., Ferrigno, C., Kuulkers, E., et al. 2017, ApJL, 848, L15
Shibata, M., Kyutoku, K., Yamamoto, T., et al. 2009, PhRvD, 79, 44030
The LIGO Scientific Collaboration, The Virgo Collaboration, Abbott, B. P.,
    et al. 2018, arXiv:1811.12907
Troja, E., Piro, L., van Eerten, H., et al. 2017, Natur, 551, 71
Villar, V. A., Guillochon, J., Berger, E., et al. 2017, ApJL, 851, L21
von Kienlin, A., Meegan, C., & Goldstein, A. 2017, GCN, 21520, 1
Wald, R. M. 1974, PhRvD, 10, 1680
Wang, J.-S., Peng, F.-K., Wu, K., et al. 2018, ApJ, 868, 19
Xiao, D., & Dai, Z. G. 2017, ApJ, 846, 130
Xiao, D., & Dai, Z. G. 2019, ApJ, 878, 62
Xiao, D., Peng, Z. K., Zhang, B.-B., & Dai, Z. G. 2018, ApJ, 867, 52
Zhang, B. 2016, ApJL, 827, L31
Zhang, B. 2019a, ApJL, 873, L9
Zhang, B. 2019b, FrPhy, 14, 64402
Zhang, B., & Yan, H. 2011, ApJ, 726, 90